# Resolving the Mixed-Alkali Effect on the Viscoelastic Behavior of Supercooled Liquids

Tae-min Yeo<sup>1,2</sup>, Bing Yuan<sup>1</sup>, Jacob Lovi<sup>1</sup>, Jung-Wook Cho<sup>2,3</sup>, Sabyasachi Sen<sup>1\*</sup>

<sup>1</sup>Deparment of Materials Science and Engineering, University of California at Davis, Davis, California 95616, USA

<sup>2</sup>Graduate Institute of Ferrous & Energy Materials Technology, Pohang University of Science and Technology (POSTECH), Pohang, 37673, Republic of Korea

<sup>3</sup>Division of Advanced Nuclear Engineering (DANE), Pohang University of Science and Technology (POSTECH), Pohang, 37673, Republic of Korea

\*Corresponding Author

E-mail: sbsen@ucdavis.edu (S. Sen)

**Abstract** 

Relaxation processes in mixed-alkali metaphosphate glasses and supercooled liquids

are studied using a combination of calorimetric, electrical impedance spectroscopic and

rheological measurements to investigate the atomistic nature of the mixed-alkali effect (MAE)

on the glass transition temperature  $T_g$  and viscous flow. While  $T_g$  and fragility index of single-

alkali liquids are controlled by the segmental motion of phosphate chains, the mixed-alkali

liquids exhibit the presence of a second relaxation process, which is slower than chain motion

and is characterized by a lower activation energy. This process is assigned to the scission and

renewal of P-O bonds that relieve the accumulated stress in the network resulting from its

matrix-mediated coupling with pairwise hopping of dissimilar alkalis. The viscous flow and

glass transition in mixed-alkali phosphate liquids appear to be controlled by this P-O bond

scission-renewal process, which is shown to be consistent with a lowering of their fragility

index and a concomitant decrease in the stretching exponent of structural relaxation, compared

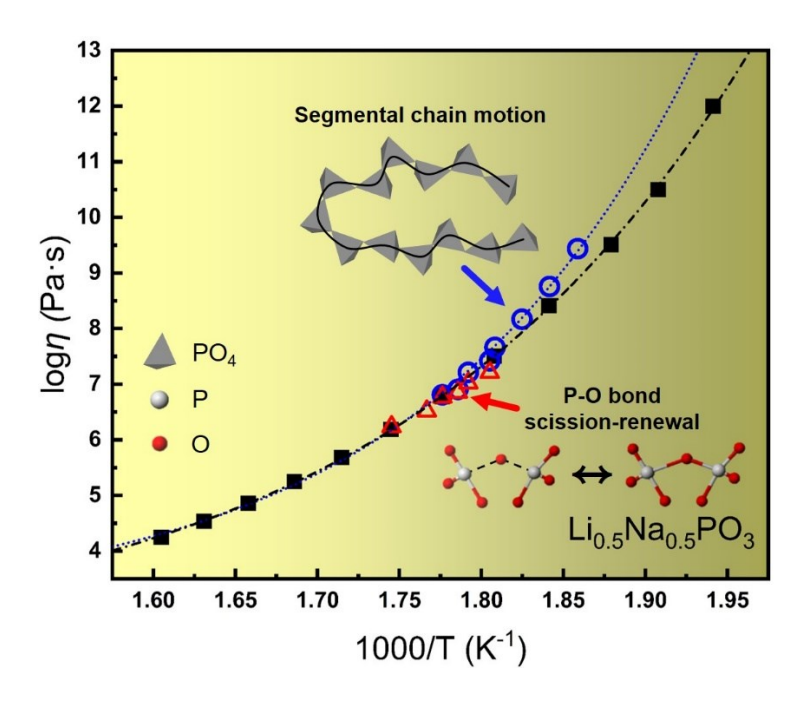
to their single-alkali counterparts.

Keywords: Mixed-alkali effect, Viscoelasticity, Glass, Supercooled Liquid, Phosphate,

Relaxation

2

# **Graphical Abstract**



#### 1. Introduction

The mixed-alkali effect (MAE) in glasses has been extensively investigated over the last several decades[1, 2]. The MAE is associated with continuous substitution of one alkali with another in a glass, which results in a strong nonlinear compositional variation in the transport properties of various glass-forming systems, most notably the ionic conductivity[3, 4]. Specifically, the ionic conductivity of a glass containing a single alkali atom type decreases upon its substitution with a second alkali atom type while the total alkali concentration is kept fixed, and the conductivity goes through a minimum near 1:1 atomic ratio of the two alkalis. It is now widely accepted that this slowdown of the motion of alkali ions results from the blocking effect of the diffusion pathway of one alkali by the other [5, 6]. This blocking effect has its origin in the site mismatch between the two alkalis, say A and B, as an A atom prefers to not hop into a site left vacant by a B atom (and vice versa) until the site is relaxed to that characteristic of A, via some local motion of the network. This site readjustment kinetics is expected to slow down with decreasing temperature and with increasing size difference between A and B, thus intensifying the MAE as has indeed been observed in experiments [3-7].

The MAE is also observed in the variation of the glass transition temperature  $T_g$  with A:B ratio, which shows a significant negative deviation from linearity in various oxide glasses[8-12]. In order to explain this negative deviation in  $T_g$ , Ingram and Roling proposed the matrix-mediated coupling (MMC) model where the size difference between the alkali cations A and B causes coupling between their movements to dissipate the mechanical stress created by A (B) cations entering sites left vacant by B (A) cations[9]. For example, the arrival of smaller (larger) Li (Na) ions to vacant sites left by Na (Li), it results in a local tensile (compressive) stress. Therefore, a coupled movement of Li and Na will result in a self-

cancelling effect of the associated tensile and compressive stress in the network that can be thought of as a mechanical dipole, and maintain an overall isochoric condition[9]. These mechanical dipoles can respond to an externally applied stress and thus give rise the strong mixed-alkali internal friction peak in the mechanical loss spectra. Although the appearance and reorientation of these mechanical dipoles due to pairwise motion of dissimilar alkali atoms are significantly faster than the structural relaxation, the repeated activity of these dipoles was hypothesized in the MMC model to have the effect of somehow loosening up the network and increasing its propensity for structural relaxation, thereby lowering the  $T_g[9]$ . However, as Ingram noted, a loosening of the network in a mixed-alkali glass is somewhat in contradiction with the concomitant slowdown of alkali motion compared to that in a single-alkali glass[13]. Changstrom and Sidebottom[12] have pointed out in support of the MMC model that both the deviation of  $T_g$  from linearity and the strength of the mixed-alkali internal friction peak in the mechanical relaxation spectra of Li<sub>x</sub>Na<sub>1-x</sub>PO<sub>3</sub> glasses associated with ionic motion show striking similarity in their dependence on the Li:Na ratio. It may be noted here that similar tensile and compressive stress distribution in the glass structure with mixed alkali cations and their reorganization have also been considered, on the basis of molecular dynamics simulations, to be responsible for the relaxation of mixed-alkali glasses at ambient temperature that gives rise to the thermometer effect[14].

Besides the MAE on  $T_g$ , a number of previous studies[8, 12, 15, 16] have shown the existence of MAE on the fragility index m of supercooled liquids, where m is a measure of the departure of the viscosity  $\eta$  of a supercooled liquid from an Arrhenius behavior and is defined as[17]:

$$m = \frac{d \log_{10} \eta}{d(T_g/T)} \bigg|_{T=T_g} \tag{1}$$

A recent study based on photon correlation spectroscopy by Changstrom and Sidebottom[12] provides detailed and clear evidence that as Li is progressively replaced by Na, the m of deeply supercooled Li<sub>x</sub>Na<sub>1-x</sub>PO<sub>3</sub> liquids goes through a minimum near a Li:Na ratio of ~ 1:1. Moreover, the dynamic structure factor S(q,t) of these liquids displayed a stretched exponential decay associated with the structural relaxation i.e.  $S(q,t) \sim \exp[-(t/\tau)^{\beta}]$ , where the stretching exponent  $\beta$  followed the same trend as m and went through a minimum near Li:Na  $\sim$  1:1. This result is in clear contradiction with the well-known inverse relation between m and  $\beta$  that has reported in the literature for a wide variety of glass-forming liquids[17]. In general m is a sensitive function of the structural connectivity in network liquids and it decreases rapidly as the phosphate chains are increasingly cross-linked upon addition of P<sub>2</sub>O<sub>5</sub> to a metaphosphate liquid[18, 19]. On the other hand, within the metaphosphate family of liquids, effective crosslinking between the phosphate chains can be altered by changing the field strength of the modifier cations[20]. Modifier cations with high field strength provides stronger effective cross-linking between the constituent phosphate chains compared to their low field strength counterparts, which in turn lowers the m of the former liquids[20]. However, the nominal connectivity of the phosphate network or the effective cross-linking between the constituent phosphate chains in metaphosphate liquids are not expected to change in a mixed-alkali series in a way that can explain the observed minimum in m. Changstrom and Sidebottom[12] proposed that the variation in m in mixed-alkali systems does not reflect a change in the cooperativity of the structural rearrangement and relaxation, but rather is an artifact of a rapid lowering of the contribution of MMC resulting from alkali motion, to structural relaxation with increasing temperature. On the other hand, Richet[21] hypothesized, on the basis of an analysis of the viscosity data of mixed-alkali silicate liquids, that it is the contribution of the mixing entropy of the alkalis towards structural relaxation that rapidly decreases with increasing temperature. Such a temperature dependence could also give rise to the observed MAE on *m*. However, the validity of these hypotheses remains to be experimentally verified.

Here, we report the results of a combined calorimetric, electrical impedance spectroscopic and rheological study of supercooled mixed-alkali metaphosphate liquids of composition  $\text{Li}_x\text{Na}_{1-x}\text{PO}_3$  with  $x=0.0,\,0.25,\,0.5,\,0.75$  and 1.0 as well as of two liquids with composition  $\text{Li}_{0.5}\text{Rb}_{0.5}\text{PO}_3$  and  $\text{Li}_{0.5}\text{K}_{0.5}\text{PO}_3$  detailing the MAE on  $T_g$ , fragility and viscoelasticity. The fundamental nature of MAE in controlling the shear relaxation behavior of these liquids is elucidated.

#### 2. Experimental procedure

## 2.1. Sample preparation

A series of mixed alkali metaphosphate of the general composition  $\text{Li}_x\text{Na}_{1-x}\text{PO}_3$  with x = 0.0, 0.25, 0.5, 0.75 and 1.0 as well as two glasses with composition  $\text{Li}_{0.5}\text{Rb}_{0.5}\text{PO}_3$  and  $\text{Li}_{0.5}\text{K}_{0.5}\text{PO}_3$  were prepared by the conventional melt-quenching method. Appropriate mixtures of reagent grade NH<sub>4</sub>H<sub>2</sub>PO<sub>4</sub> (99.99%, Acros Organics), Li<sub>2</sub>CO<sub>3</sub> (99.999%, Alfa Aesar), Na<sub>2</sub>CO<sub>3</sub> (99.999%, Alfa Aesar), K<sub>2</sub>CO<sub>3</sub> (99.999%, Alfa Aesar) and Rb<sub>2</sub>CO<sub>3</sub> (99.999%, Alfa Aesar) were mixed in a quartz crucible. The mixtures were calcinated at 450 °C for 17 h to remove H<sub>2</sub>O, NH<sub>3</sub>, and CO<sub>2</sub> and were subsequently melted in air at 1100 °C for 1 h followed by quenching on a graphite plate. The glass samples were immediately transferred into a vacuum desiccator to avoid their exposure to atmospheric moisture until further measurements.

# 2.2. Thermophysical characterization

The fictive temperature  $T_f$  of these glasses and its dependence on the cooling/heating rate were measured using differential scanning calorimetry (DSC) (Mettler Toledo DSC1). For each glass composition, approximately 15 to 25 mg of sample was taken in hermetically sealed

Al pans. The samples were heated at a specific rate of q K/min under a nitrogen atmosphere to 30 K above  $T_g$  to erase any thermal history, cooled down to  $T_g - 50$  K and then reheated at the same rate. The  $T_f$  is taken as the onset of the endothermic glass transition signal during reheating and was measured as a function of q ranging between 0.5 and 30 K/min.  $T_g$  was taken as the  $T_f$  obtained at a heating/cooling rate of q = 10 K/min. The estimated error in  $T_f$  is within  $\pm 2$  K.

## 2.4. Electrical Impedance Spectroscopy

Small disks of the  $\text{Li}_x \text{Na}_{I\to x} \text{PO}_3$  glass samples were polished and  $\sim 50$  nm thick gold electrodes were sputtered to the two parallel faces of the sample after dry-polishing with 2400 grit sandpaper, for electrical impedance spectroscopy (EIS). The impedance measurements were carried out under air in the temperature range of 25 - 300 °C, using a Novocontrol Alpha – AN modulus analyzer in the frequency range of  $10^{-1} - 10^7$  Hz. The fittings of the measured impedance spectra with an appropriate equivalent circuit model were performed using the software Z-View. The frequency dependent conductivity  $\sigma(\omega)$  is computed using the values of the real and imaginary parts of the impedance,  $Z'(\omega)$  and  $Z''(\omega)$ , respectively, as obtained from EIS measurements and using the relation:  $\sigma(\omega) = \frac{1}{\sqrt{Z'(\omega)^2 + Z''(\omega)^2}} \left(\frac{L}{A}\right)$  where L and A denote the sample thickness (1-2 mm) and the electrode area ( $\sim 20$  mm²), respectively. The real and imaginary parts of the dielectric constant  $\varepsilon'(\omega)$  and  $\varepsilon''(\omega)$ , as obtained from EIS measurements are used to calculate the real and imaginary parts of the electric modulus  $M'(\omega)$  and  $M''(\omega)$  utilizing the relations:  $M' = \frac{\varepsilon'(\omega)}{\varepsilon'^2(\omega) + \varepsilon'^2(\omega)}$  and  $M''' = \frac{\varepsilon''(\omega)}{\varepsilon'^2(\omega) + \varepsilon'^2(\omega)}$ .

#### 2.4. Rheological Characterization

The steady and small angle oscillatory shear (SAOS) rheological measurements of these supercooled metaphosphate liquids were carried out using a parallel plate rheometer (MCR302, Anton-Paar) under an environment of flowing nitrogen gas. The temperature of the sample was controlled by a convection oven (up to 600 °C). The glass samples were heated above the softening point to reach a viscosity of  $\sim 10^5$  Pa·s and trimmed between the two plates to form a sandwich-like geometry with a gap of ~ 1 mm. At each desired measurement temperature, the samples were allowed to equilibrate and subsequently subjected to a sinusoidal strain with varying angular frequency ω between 1 to 628 rad/s and the induced torque was recorded to calculate the storage and loss moduli G' and G'' as a function of  $\omega$ . The upper plate (8 mm diameter, stainless steel) was used to apply the sinusoidal strain while the nonremovable lower plate (25 mm diameter, stainless steel) remained stationary. The corresponding stress response was recorded using a torque transducer. The applied strain of all oscillatory shear measurements was controlled within a predetermined linear viscoelastic region. Master curves of G' and G'' were obtained using time-temperature superposition (TTS). The Newtonian viscosity  $\eta$  of these liquids in the range  $\sim 10^4$  -  $10^9$  Pa·s was measured under steady shear, where the viscosity was determined as the ratio of stress and strain rate at various shear rates  $\dot{\gamma}$  ranging between 0.01 s<sup>-1</sup> and 1 s<sup>-1</sup> at each temperature. The viscosity in the range  $\sim 10^{9.5}$ - $10^{11}$  Pa·s was measured using creep test using the same rheometer setup. In the creep test, the strain was recorded as a function of time while the sample was kept under a constant shear stress  $\tau$ . The strain profile exhibits a linear region at longer times corresponding to the steady state viscous response of the material, where the gradient of this region yields the strain rate  $\dot{\gamma}$ , and consequently the viscosity  $\eta$  could be obtained from the relation:  $\eta = \frac{\tau}{\dot{\gamma}}$  [22]. Detailed information on the experimental setup for these rheometric measurements and data analysis procedure can be found in previous publications[23, 24].

#### 3. Results

#### 3.1. Calorimetric glass transition and electrical conductivity

The DSC scans and the calorimetric  $T_g$  for the  $\text{Li}_x \text{Na}_{1-x} \text{PO}_3$  glasses studied here are shown in Fig. 1. The  $T_g$  data are consistent with those reported in previous studies and the mixed alkali glasses display the expected non-linear variation of  $T_g$  with the Li:Na ratio, which goes through a minimum near the 50:50 composition [8]. The dc conductivity of these glasses is shown in Fig. 2. The activation energies and conductivity are also consistent with previous reports in the literature[25-27] on similar compositions and show the typical mixed-alkali effect of the drastic lowering of conductivity on replacing Li (Na) with Na (Li), which goes through a minimum near the 50:50 composition (Fig. 2). The activation energy of ionic conduction shows the expected increase for the mixed-alkali compositions compared to the single-alkali end members (Fig. 2). The corresponding temperature dependence of the conductivity relaxation time for these glasses can be obtained from the impedance spectra using the modulus representation (Fig. 3). In this representation the peak frequency  $f_{max}$  of the imaginary part of the electric modulus M'' is related to the most probable conductivity relaxation time  $\tau_{cond}$  as:  $\tau_{cond} = \frac{1}{2\pi f_{max}}$  [28].

### 3.2. Viscosity and kinetic fragility

The q dependence of  $T_f$  for these glasses is shown Fig. 4. In all cases  $1/T_f$  displays a linear dependence on  $\ln q$ , as q is varied over nearly two orders of magnitude from 0.5 K/min to 40 K/min. The activation energy  $E_g$  for enthalpy relaxation can be determined from the slope of this linear variation as [29]:

$$\frac{dlnq}{d\left(\frac{1}{T_f}\right)} = -\frac{E_g}{R} \tag{2}$$

The calorimetric fragility  $m_c$  can then be obtained from  $E_g$  using the relation [30]:

$$m_c = \frac{E_g}{RT_g \ln 10} \tag{3}$$

The temperature dependence of the viscosity  $\eta$  of these Li<sub>x</sub>Na<sub>1-x</sub>PO<sub>3</sub> liquids as obtained from steady shear parallel plate rheometry is shown in Fig. 5. The corresponding variation in the isokom temperatures as a function of alkali composition is shown in Fig. 6. As expected, the composition dependence of the high-viscosity ( $\eta > 10^7$  Pa.s) isokom temperatures shows a clear MAE with a minimum near the 50:50 composition but the effect becomes weaker at lower viscosities such that the minimum nearly disappears for  $\eta < 10^6$  Pa.s (Fig. 6). These viscosity data are fitted to the standard Mauro-Yue-Ellison-Gupta-Allan (MYEGA) equation (Eqn. 4) to obtain the kinetic fragility index  $m_k$  for each liquid [31]. The MYEGA equation can be written as:

$$\log \eta = \log \eta_{\infty} + (12 - \log \eta_{\infty}) \cdot \frac{T_g}{T} \cdot \exp \left[ \left( \frac{m_k}{12 - \log \eta_{\infty}} - 1 \right) \cdot \left( \frac{T_g}{T} - 1 \right) \right] \tag{4}$$

where  $\log \eta_{\infty}$  and  $m_k$  are adjustable fitting parameters and  $T_g$  is the calorimetrically determined glass transition temperature. These fits of the MYEGA equation to the viscosity data are shown on a  $T_g/T$  plot in Fig. 7. It may be noted here that the kinetic fragility index  $m_k$  is equivalent to fragility index defined in Eqn. 1 above as  $m = \frac{dlog\eta(T)}{d(T_g/T)}\Big|_{T=T_g}$ . The compositional variation of the fragility indices  $m_c$  and  $m_k$  of these Li<sub>x</sub>Na<sub>1-x</sub>PO<sub>3</sub> liquids, thus obtained from Eqns. 3 and 4, are shown in Fig. 8. Although the values of  $m_c$  and  $m_k$  obtained using different techniques are somewhat different, both follow similar non-monotonic trends with composition, with mixed alkali glasses being characterized by lower values of these indices, compared to the single-alkali end members. Both  $m_c$  and  $m_k$  go through a minimum near the Li:Na = 50:50 composition and the values for  $m_c$  are in reasonably good agreement

with the fragility indices for the structural relaxation of Li<sub>x</sub>Na<sub>1-x</sub>PO<sub>3</sub> liquids measured in a previous study using photon correlation spectroscopy[12].

#### 3.3. Shear mechanical response

The temperature-dependent evolution of the G' and G" spectra of Li<sub>x</sub>Na<sub>1-x</sub>PO<sub>3</sub> liquids with x = 0.0, 0.5 and 1.0 are shown in Fig. 9. It may be noted that within the frequency window of observation that is characteristic of the rheometer, only a portion of the whole spectrum is revealed at any specific temperature. The high (low) frequency region is revealed at low (high) temperature, thus enabling a sequential observation of a wide frequency range via variation in temperature. The experimental master curves of the storage and loss shear moduli  $G'(\omega)$  and  $G''(\omega)$  can then be constructed using time-temperature superposition (TTS). These master curves of Li<sub>x</sub>Na<sub>1-x</sub>PO<sub>3</sub> liquids constructed using TTS at temperatures corresponding to a viscosity of ~10<sup>7</sup> Pa·s are shown in Fig. 10. The single-alkali LiPO<sub>3</sub> and NaPO<sub>3</sub> liquids display a "simple" behavior consistent with a single most probable relaxation time  $\tau_R$ corresponding to a G'-G" crossover at a frequency  $\omega = 2\pi\tau_R^{-1}$  where G" goes through a maximum and a Maxwell scaling of G ( $\omega$ )  $\sim \omega^n$  at low frequencies, with n=2 and 1 for G' and G", respectively. At higher frequencies beyond the crossover G' reaches the glassy plateau value of G<sub>∞</sub> (Fig. 10). However, the viscoelastic spectrum of the mixed alkali Li<sub>0.5</sub>Na<sub>0.5</sub>PO<sub>3</sub> liquid shows a different behavior with both G' and G" displaying a clear change in slope from Maxwell scaling at intermediate frequencies below the crossover. Such a behavior is also displayed by the Li<sub>0.5</sub>K<sub>0.5</sub>PO<sub>3</sub> and Li<sub>0.5</sub>Rb<sub>0.5</sub>PO<sub>3</sub> mixed-alkali liquids (Fig. 11) and can be simulated well with two distinct relaxation processes in these liquids that are characterized by significantly different timescales and  $G_{\infty}$  values (Figs. 10, 11).

#### 4. Discussion

As noted above, the non-monotonic negative deviation of  $T_g$  of the mixed alkali glasses from the linear trend joining the single-alkali end members in the series was attributed by Ingram and coworkers[9, 13] to a matrix-mediated coupling of the appearance and isochoric repositioning of mechanical dipoles in the network induced by pairwise hopping of dissimilar alkali ions. Mixing cations triggers isochoric mechanical flexing in the network due to the swapping of regions of compression and tension around alkalis of dissimilar sizes as they perform hopping dynamics, which loosens and softens the network, resulting in the depression of  $T_g$ . Although such dynamical processes could potentially increase the network's propensity for relaxation, considering the large temporal decoupling between the relatively fast motion of mechanical dipoles and the slow structural and shear relaxation that is characteristic of the network liquids near  $T_g$ , a clear mechanistic connection between the two processes remains to be established. This temporal decoupling in the case of Li<sub>x</sub>Na<sub>1-x</sub>PO<sub>3</sub> liquids is evident in Fig. 12, where the  $\tau_{cond}$  of these glasses measured using electrical impedance spectroscopy is compared with the shear relaxation timescale  $\tau_{shear}$  of the corresponding liquids. Here  $\tau_{shear}$  was obtained from the viscosity data in Fig. 5, using the Maxwell relation  $\tau_{shear}$  =  $\eta/G_{\infty}$ . It is clear from Fig. 12 that although, compared to the single-alkali glasses, the magnitude of this temporal decoupling is lower in the case of mixed-alkali glasses,  $\tau_{shear}$  is still several orders of magnitude slower than  $\tau_{cond}$  in the latter. It may be noted here that for the single-alkali LiPO<sub>3</sub> and NaPO<sub>3</sub> glasses the activation energy and relative magnitude of  $\tau_{cond}$  agree well with the relaxation timescale obtained from the internal friction data reported in previous studies (Fig. 12) [27]. On the other hand, for the mixed-alkali Li<sub>0.5</sub>Na<sub>0.5</sub>PO<sub>3</sub> glass only the activation energy of the mixed-alkali internal friction peak (~ 113 kJ/mol) is in agreement with that ( $\sim 112$  kJ/mol) of  $\tau_{cond}$ , while the timescale of the former is significantly

longer than that of the latter (Fig. 12). This mixed-alkali internal friction peak has been tentatively associated with the pairwise hopping of dissimilar alkali motion, responsible for the MMC. Therefore, it is clear from Fig. 12 that the  $\tau_{shear}$  of all Li<sub>x</sub>Na<sub>1-x</sub>PO<sub>3</sub> glasses display a rather large temporal decoupling of several orders of magnitude from all alkali motion including single and pairwise alkali hopping in the glass transition range (Fig. 12)[27].

It may be noted that within the framework of this MMC model one may expect the negative deviation in the compositional variation of  $T_g$  to be more pronounced in mixed-alkali glasses with larger size difference between the two alkalis as alkali hopping in these glasses would lead to a more pronounced network stress redistribution. This hypothesis is tested in Fig. 13 where the negative deviation of  $T_g$  from a linear trend is shown for Li<sub>0.5</sub>X<sub>0.5</sub>PO<sub>3</sub> [X = Na, K, Rb] glasses measured in this study along with that for mixed-alkali silicate and borate glasses reported in previous studies in the literature [10, 11]. It is clear from Fig. 13 that the magnitude of the negative deviation in  $T_g$  does not monotonically increase with increasing size difference between the two alkali ions, but it is maximized near an intermediate alkali radius ratio of  $\sim 1.4$  for the phosphate and silicate systems and  $\sim 1.7$  for the borate system. The lowering of the  $T_g$  deviation for large size difference between the alkalis is, however, not inconsistent with the MMC model if one considers that the difference in the hopping frequency between the two alkali atoms will increase with increasing size difference. Consequently, events of near-simultaneous hopping of a pair of small and large cation that is required for an isochoric flexing of the network will be increasingly less frequent with increasing size difference, leading to a lower deviation in  $T_g$  from the linear trend. In a recent study it has been hypothesized that the lower fragility index of mixed-alkali liquids, compared to that of the single-alkali end members, is a consequence of the progressively smaller contribution of this isochoric network flexing process towards viscosity and shear relaxation with increasing temperature beyond  $T_g[12]$ .

When taken together, this scenario of the MAE on  $T_g$  and fragility index indicates that the shear or structural relaxation near the glass transition in a mixed-alkali glass may be controlled by a process that is distinct from the regular mode of shear or structural relaxation, which in metatphosphate liquids involves the segmental motion of the constituent phosphate chains of corner shared PO<sub>4</sub> tetrahedra [32]. Indeed, the viscoelastic spectra of all three  $Li_{0.5}X_{0.5}PO_3$  [X = Na, K, Rb] mixed-alkali liquids display the presence of two distinct relaxation processes as opposed to a single process in the single-alkali liquids (Figs. 9-11). The relaxation time  $\tau_R$  for the latter process in the single-alkali liquids, as obtained from the G'-G" crossover frequency in their viscoelastic spectra show excellent agreement with the  $\tau_{shear}$  (Fig. 14). On the other hand, the relaxation time  $\tau_R^{fast}$  of the "fast" process in the viscoelastic spectrum of the mixed-alkali liquids agrees well with  $\tau_{shear}$  at high temperatures. The  $G_{\infty}$  of this process is on the order of  $\sim 2$  GPa, which is similar to that characteristic of the relaxation process of the single-alkali liquids, and thus can be assigned to the segmental dynamics of the phosphate chains. However, cooling results in an onset of decoupling of this process from shear relaxation such that the shear relaxation gets progressively faster i.e.  $\tau_{shear} < \tau_R^{fast}$  (Fig. 14). In contrast to the "fast" process characterized by a relatively high activation energy (619  $\pm$  23 kJ/mol), the "slow" process with a lower activation energy (301  $\pm$ 28 kJ/mol) shows an increased temporal coupling with the shear relaxation on lowering of temperature towards  $T_g$  i.e.  $\tau_R^{slow}$  approaches  $\tau_{shear}$  (Fig. 14). Although such data could only be obtained over a relatively small range of timescales limited by the frequency window of shear-mechanical spectroscopy, it is clear from Fig. 14 that owing to its lower activation energy the "slow" process would eventually become faster than the "fast" process with further

lowering of temperature as the glass transition is approached. Therefore, near the glass transition the viscous flow and shear relaxation in mixed-alkali phosphate liquids appear to be controlled by a dynamical process that is different from and faster than the segmental motion of phosphate chains. Based on the above discussion we argue that this relaxation process results from the matrix-mediated coupling of the phosphate network with the pairwise motion of dissimilar alkali ions in mixed-alkali liquids. Considering the similarity of the activation energy of this process (301  $\pm$  28 kJ/mol) to the energy of P-O bonds in oxides ( $\sim$  350 kJ/mol) [32], we argue that it represents local structural adjustments involving the scission and renewal of P-O bonds that relieve the stress accumulated over many cycles of the appearance and reorientation of the mechanical dipoles associated with pairwise alkali hopping with imperfect conservation of volume. It may be noted that the  $G_{\infty}$  of this relaxation process is on the order of ~ 0.1 GPa, which is an order of magnitude lower than that characteristic of the chain dynamics. The predicted viscosity of the Li<sub>0.5</sub>Na<sub>0.5</sub>PO<sub>3</sub> liquid from this process, as calculated using the Maxwell relation  $\eta = \tau \cdot G_{\infty}$ , is shown in Fig. 15. The importance of this process in controlling the viscous flow at temperatures close to the glass transition range is again clear in Fig. 15 and the lower activation energy of this P-O bond scission-renewal process compared to that of the phosphate chain dynamics is consistent with the observation that the mixed-alkali liquids are characterized by lower fragility indices compared to their single-alkali counterparts. Intriguingly, the data in Fig. 15 suggests that both dynamical processes contribute to viscosity at high temperatures where viscosity is lower than 10<sup>7</sup> Pa.s, at which point the MAE on viscosity also disappears (Fig. 6).

Finally, we consider the observation made by Changstrom and Sidebottom[12] of a simultaneous lowering of the structural relaxation stretching exponent  $\beta$  along with m in mixed-alkali Li<sub>x</sub>Na<sub>1-x</sub>PO<sub>3</sub> liquids, compared to those shown by the Li and Na end members. The

stretching exponent  $\beta$  ranges between 0 and 1 and is an indicator of dynamical heterogeneity such that a lower value of  $\beta$  corresponds to a wider distribution of relaxation timescales. Although a simultaneous lowering of  $\beta$  and m may appear to be anomalous as a vast variety of glass-forming liquids display a negative correlation between these two quantities[17], such a result is in fact consistent with the relaxation model proposed here for the mixed-alkali liquids. While the structural relaxation in the single-alkali Li and Na metaphosphate liquids is primarily associated with the segmental dynamics of the phosphate chains, that in the mixed-alkali liquids appears to involve a second process of P-O bond scission-renewal with a relatively low activation energy, in addition to the chain dynamics. Together, these two processes cover a wide range of timescales, which is manifested in the lower  $\beta$  value of the mixed-alkali liquids. On the other hand, the shear relaxation and thus m in these liquids is controlled predominantly by the low-activation-energy P-O bond scission-renewal process.

#### 5. Conclusions

The shear mechanical response of supercooled  $Li_xNa_{1-x}PO_3$ ,  $Li_{0.5}Rb_{0.5}PO_3$  and  $Li_{0.5}K_{0.5}PO_3$  liquids reveal the atomistic nature of the MAE on  $T_g$ , fragility and viscous flow. Shear relaxation in single-alkali liquids is controlled by the segmental motion of the constituent phosphate chains. In addition to the chain motion, the mixed alkali Li-Na, Li-K and Li-Rb metaphosphate liquids all display the presence of a second relaxation process. In the temperature range of observation the timescale of this process is significantly slower and its activation energy is nearly a factor of two lower than those characteristic of the chain motion. Although this activation energy of the slow dynamical process likely increases at lower temperatures due to increasing cooperativity, its high-temperature value of  $\sim 300 \text{ kJ/mol}$  obtained in this study likely corresponds to the elementary step and compares well with the P-

O bond energy reported in the literature. We hypothesize that this dynamical process is associated with the scission and renewal of P-O bonds in the network, which release the stress that gets accumulated from multiple events of pairwise hopping of dissimilar alkalis, a process that is an essential ingredient of the MMC model proposed by Ingram and Roling to explain the MAE on  $T_g$ . The P-O bond scission-renewal process is shown to control the viscous flow and glass transition of mixed-alkali phosphate liquids and its low activation energy naturally explains the lower fragility index m of these liquids compared to those characteristic of their single-alkali counterparts. Furthermore, unlike the single-alkali liquids, the presence of multiple relaxation processes in mixed-alkali liquids results in a broader distribution of structural relaxation timescales in the latter. This broadening of the distribution of relaxation timescales in mixed-alkali liquids is manifested in an increased stretching of the decay of the dynamic structure factor with the stretching exponent  $\beta$  displaying MAE.

## Acknowledgments

This work was supported by an NSF grant (DMR 1855176) to SS. Tae-min Yeo acknowledges support from Korea Institute for Advancement of Technology(KIAT) grant funded by the Korea Government(MOTIE) (P0017304, Human Resource Development Program for Industrial Innovation).

#### References

- [1] D.E. Day, Mixed alkali glasses—their properties and uses, Journal of Non-Crystalline Solids 21(3) (1976) 343-372.
- [2] A. Atila, Y. Ouldhnini, S. Ouaskit, A. Hasnaoui, Atomistic insights into the mixed-alkali effect in phosphosilicate glasses, Physical Review B 105(13) (2022) 134101.
- [3] M.D. Ingram, Ionic conductivity and glass structure, Philosophical Magazine B 60(6) (1989) 729-740.
- [4] H. Jain, H.L. Downing, N.L. Peterson, The mixed alkali effect in lithium-sodium borate glasses, Journal of non-crystalline solids 64(3) (1984) 335-349.
- [5] J. Swenson, A. Matic, C. Karlsson, L. Börjesson, C. Meneghini, W. Howells, Random ion distribution model: A structural approach to the mixed-alkali effect in glasses, Physical Review B 63(13) (2001) 132202.
- [6] A. Bunde, M.D. Ingram, P. Maass, The dynamic structure model for ion transport in glasses, Journal of non-crystalline solids 172 (1994) 1222-1236.
- [7] P. Maass, A. Bunde, M.D. Ingram, Ion transport anomalies in glasses, Physical review letters 68(20) (1992) 3064.
- [8] P.F. Green, E.F. Brown, R.K. Brow, Dynamics of mixed alkali metaphosphate glasses and liquids, Journal of non-crystalline solids 255(1) (1999) 87-96.
- [9] M.D. Ingram, B. Roling, The concept of matrix-mediated coupling: a new interpretation of mixed-cation effects in glass, Journal of Physics: Condensed Matter 15(16) (2003) S1595.
- [10] J.E. Shelby, Thermal expansion of mixed-alkali silicate glasses, Journal of Applied Physics 47(10) (1976) 4489-4496.
- [11] C.M. Kuppinger, J.E. Shelby, Viscosity and thermal expansion of mixed-alkali borate glasses, Journal of the American Ceramic Society 69(12) (1986) C-292-C-293.
- [12] J.R. Changstrom, D.L. Sidebottom, Study of the mixed alkali effect in lithium and sodium metaphosphate glass-forming liquids by photon correlation spectroscopy, Journal of Physics: Condensed Matter 20(28) (2008) 285103.
- [13] M.D. Ingram, J.E. Davidson, A.M. Coats, E.I. Kamitsos, J.A. Kapoutsis, Glass Sci. Technol, Glastech. Ber 67 (1994) 151-55.
- [14] Y. Yu, M. Wang, M.M. Smedskjaer, J.C. Mauro, G. Sant, M. Bauchy, Thermometer effect: origin of the mixed alkali effect in glass relaxation, Physical review letters 119(9) (2017) 095501.
- [15] K. Putz, P.F. Green, Fragility in mixed alkali tellurites, Journal of non-crystalline solids 337(3) (2004) 254-260.
- [16] J. Kjeldsen, M.M. Smedskjaer, J.C. Mauro, Y. Yue, On the origin of the mixed alkali effect on indentation in silicate glasses, Journal of non-crystalline solids 406 (2014) 22-26.
- [17] R. Böhmer, K.L. Ngai, C.A. Angell, D.J. Plazek, Nonexponential relaxations in strong and fragile glass formers, The Journal of chemical physics 99(5) (1993) 4201-4209.

- [18] D.L. Sidebottom, Fragility of network-forming glasses: A universal dependence on the topological connectivity, Physical Review E 92(6) (2015) 062804.
- [19] D.L. Sidebottom, T. Tran, S. Schnell, Building up a weaker network: the effect of intermediate range glass structure on liquid fragility, Journal of non-crystalline solids 402 (2014) 16-20.
- [20] Y. Xia, W. Zhu, M. Lockhart, B. Aitken, S. Sen, Fragility and rheological behavior of metaphosphate liquids: Insights into their chain vs. network characters, Journal of Non-Crystalline Solids 514 (2019) 77-82.
- [21] P. Richet, Viscosity and configurational entropy of silicate melts, Geochimica et Cosmochimica Acta 48(3) (1984) 471-483.
- [22] Y. Xia, B. Yuan, O. Gulbiten, B. Aitken, S. Sen, Kinetic and calorimetric fragility of chalcogenide glass-forming liquids: Role of shear vs enthalpy relaxation, The Journal of Physical Chemistry B 125(10) (2021) 2754-2760.
- [23] S. Sen, W. Zhu, B. Aitken, Behavior of a supercooled chalcogenide liquid in the non-Newtonian regime under steady vs. oscillatory shear, The Journal of Chemical Physics 147(3) (2017) 034503.
- [24] W. Zhu, B. Aitken, S. Sen, Structural mechanism of iodine incorporation in As-Se-I glasses and its effects on physical properties, Journal of Non-Crystalline Solids 478 (2017) 79-84.
- [25] S.W. Martin, C.A. Angell, DC and AC conductivity in wide composition range Li2O · P2O5 glasses, Journal of Non-Crystalline Solids 83(1-2) (1986) 185-207.
- [26] J.E. Tsuchida, F.A. Ferri, P.S. Pizani, A.C.M. Rodrigues, S. Kundu, J.F. Schneider, E.D. Zanotto, Ionic conductivity and mixed-ion effect in mixed alkali metaphosphate glasses, Physical Chemistry Chemical Physics 19(9) (2017) 6594-6600.
- [27] H. Van Ass, J. Stevels, Internal friction of mixed alkali metaphosphate glasses:(I). Results, Journal of Non-Crystalline Solids 15(2) (1974) 215-238
- [28] K. Pathmanathan, J.R. Stevens, Improved analysis of ionic conductivity relaxation using the electric modulus with a Cole-Davidson distribution, Journal of Applied Physics 68(10) (1990) 5128-5132.
- [29] D.L. Sidebottom, D. Vu, Assessing the network connectivity of modifier ions in metaphosphate glass melts: A dynamic light scattering study of Na-Zn mixtures, The Journal of Chemical Physics 145(16) (2016) 164503.
- [30] K.F. Kelton, Kinetic and structural fragility—a correlation between structures and dynamics in metallic liquids and glasses, Journal of Physics: Condensed Matter 29(2) (2016) 023002.
- [31] J.C. Mauro, Y. Yue, A.J. Ellison, P.K. Gupta, D.C. Allan, Viscosity of glass-forming liquids, Proceedings of the National Academy of Sciences 106(47) (2009) 19780-19784.
- [32] Y. Xia, W. Zhu, J. Sen, S. Sen, Observation of polymer-like flow mechanism in a short-chain phosphate glass-forming liquid, The Journal of Chemical Physics 152(4) (2020) 044502.
- [33] Y. Xia, H. Chen, B. Aitken, S. Sen, Rheological characterization of complex dynamics in Na–Zn metaphosphate glass-forming liquids, The Journal of Chemical Physics 155(5) (2021) 054503.

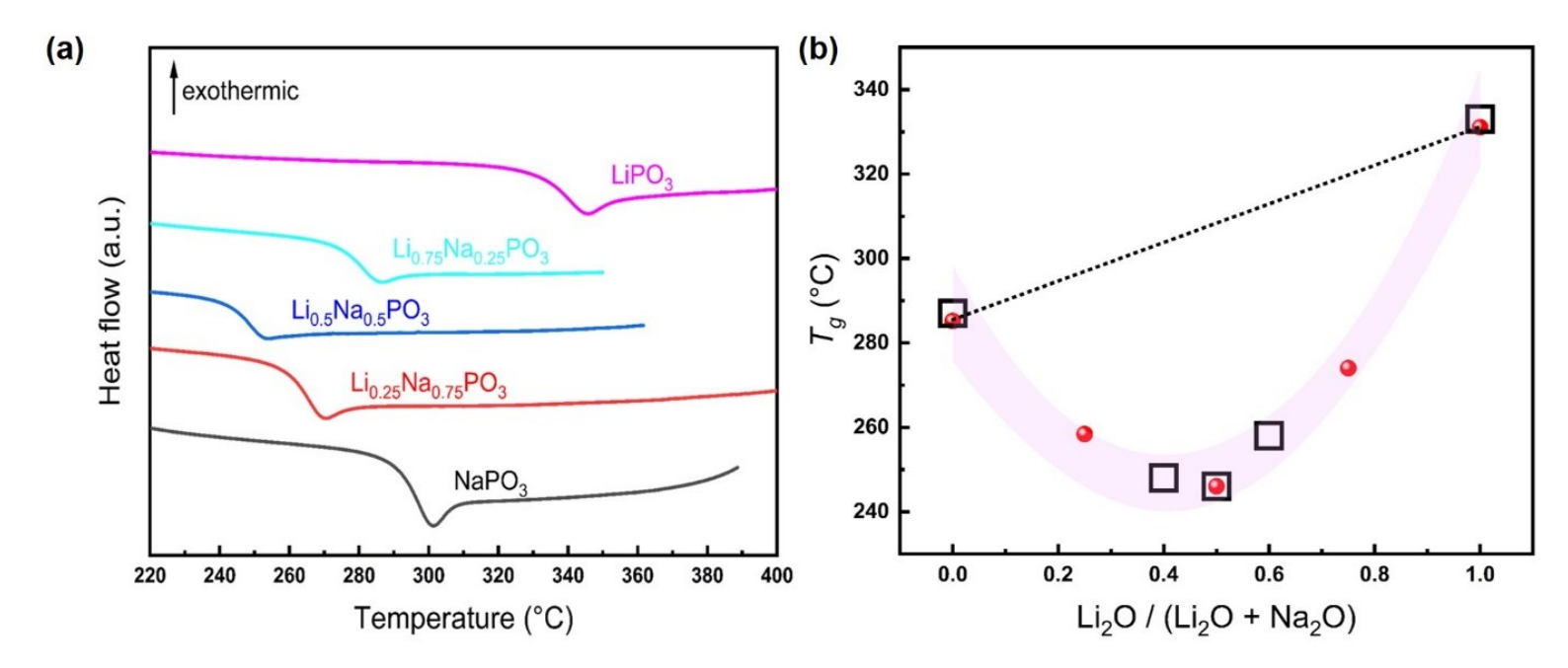
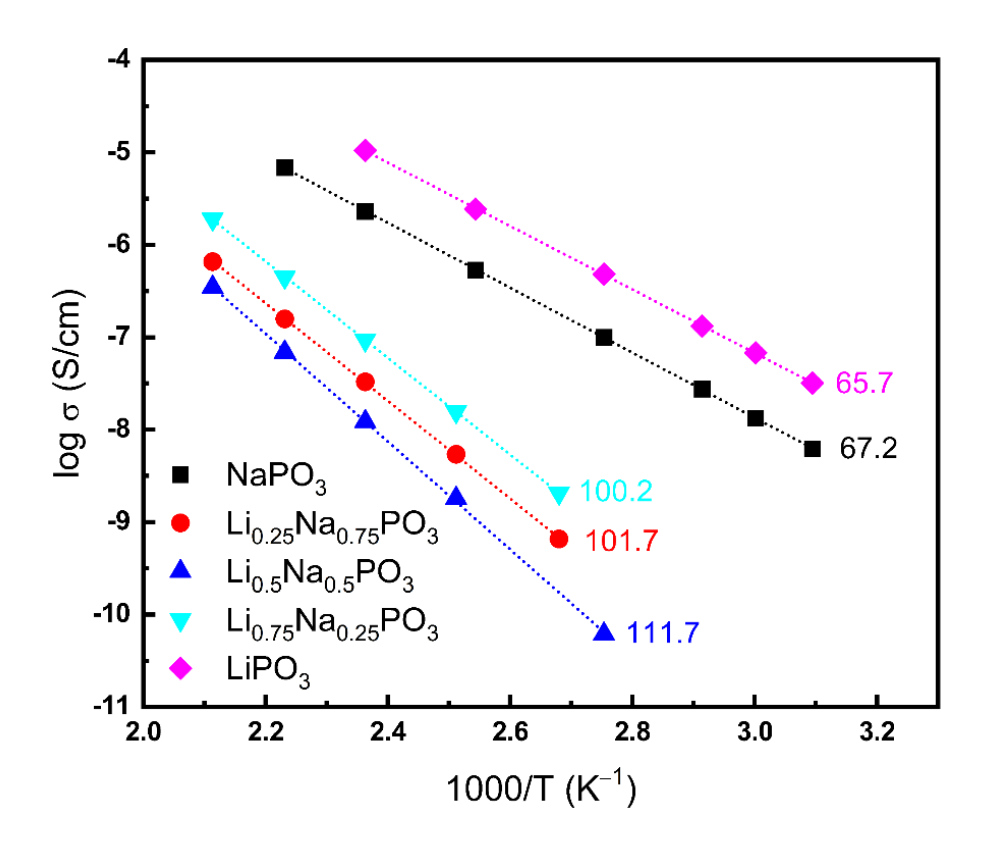


Fig. 1. (a) DSC scans and (b) variation of glass transition temperature  $T_g$  for Li<sub>x</sub>Na<sub>1-x</sub>PO<sub>3</sub> glasses. Red circles in (b) are  $T_g$  measured in present study and open black squares are data from Green *et al*[8]



**Fig. 2.** Temperature dependence of conductivity  $\sigma$  of Li<sub>x</sub>Na<sub>1-x</sub>PO<sub>3</sub> glasses. Dotted lines through the datapoints are linear least-squares fits. Activation energy for each composition in kJ/mol is listed alongside the corresponding conductivity curve.

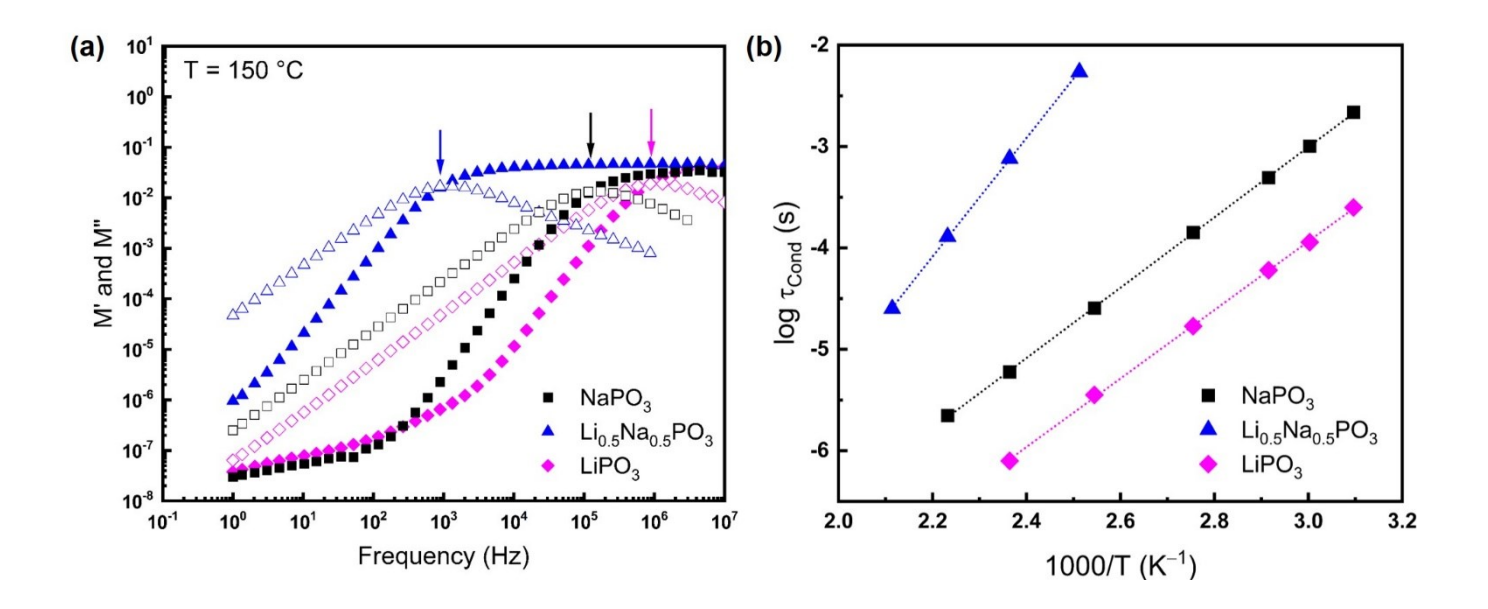
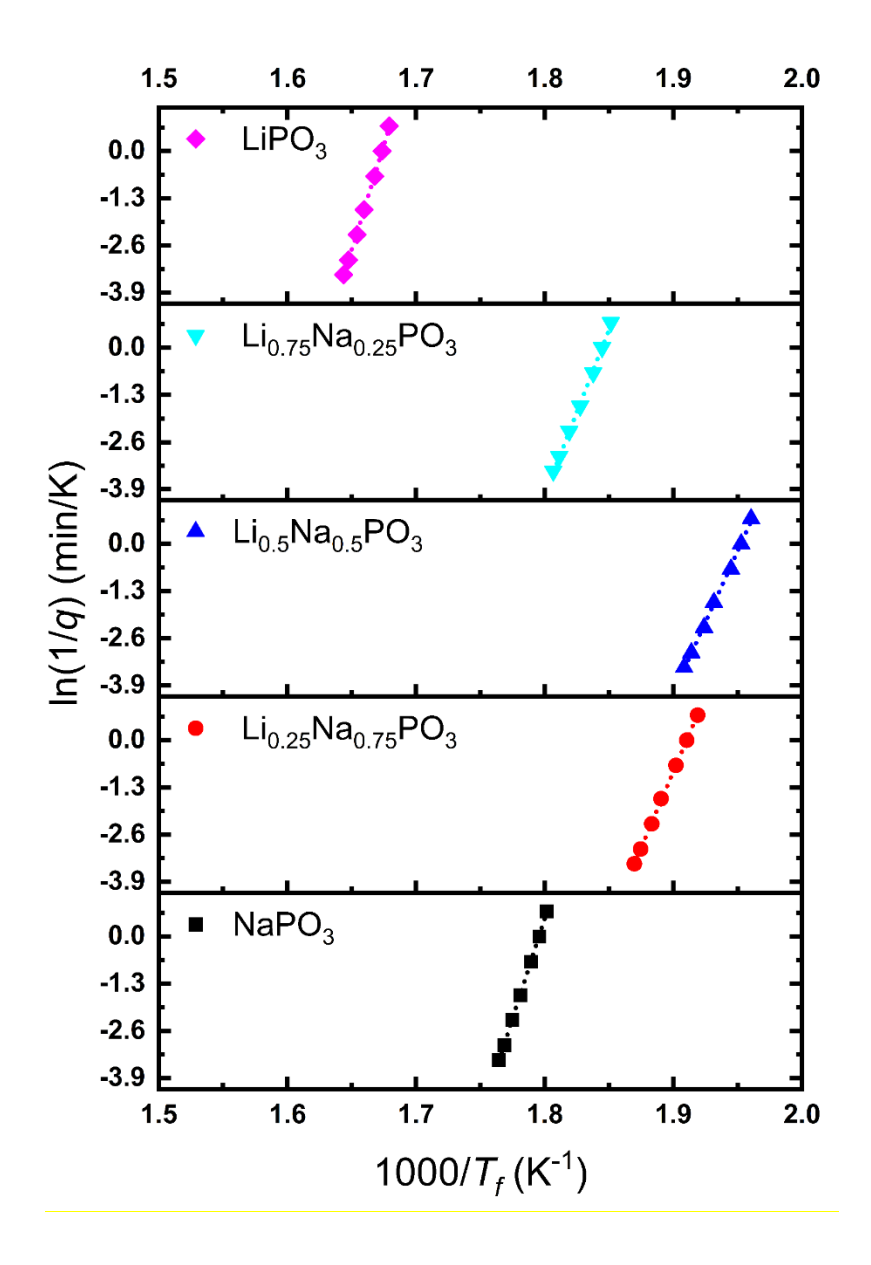
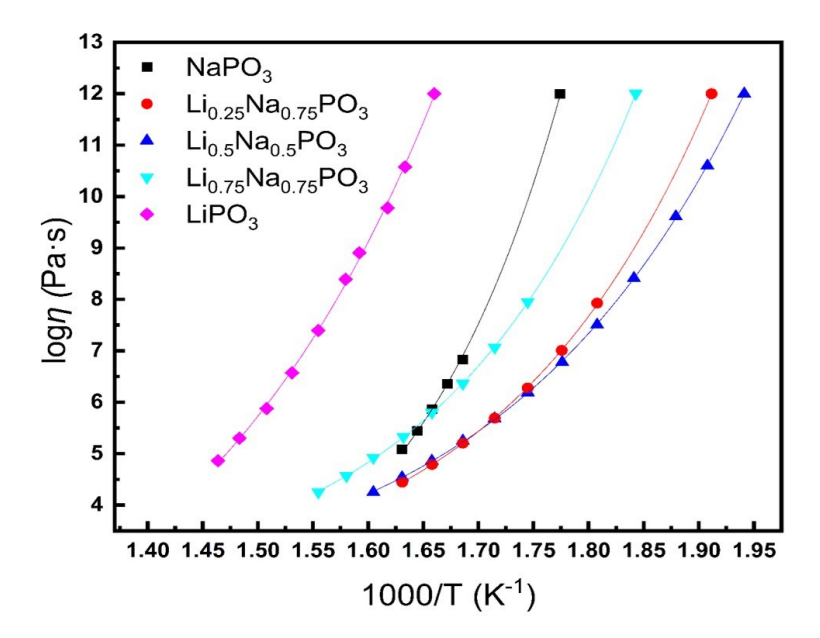


Fig. 3. (a) Frequency dependence of M' (solid symbols) and M'' (open symbols) at 150 °C and (b) temperature dependence of conductivity relaxation time  $\tau_{cond}$  of Li<sub>x</sub>Na<sub>1-x</sub>PO<sub>3</sub> glasses. Arrows indicate M'-M'' crossover points used to determine  $\tau_{cond}$ .



**Fig. 4**. Heating rate q vs. fictive temperature  $T_f$  of Li<sub>x</sub>Na<sub>1-x</sub>PO<sub>3</sub> glasses.



**Fig. 5.** Temperature dependence of viscosity of Li<sub>x</sub>Na<sub>1-x</sub>PO<sub>3</sub> liquids. Solid lines are fits of MYEGA equation to experimental data.

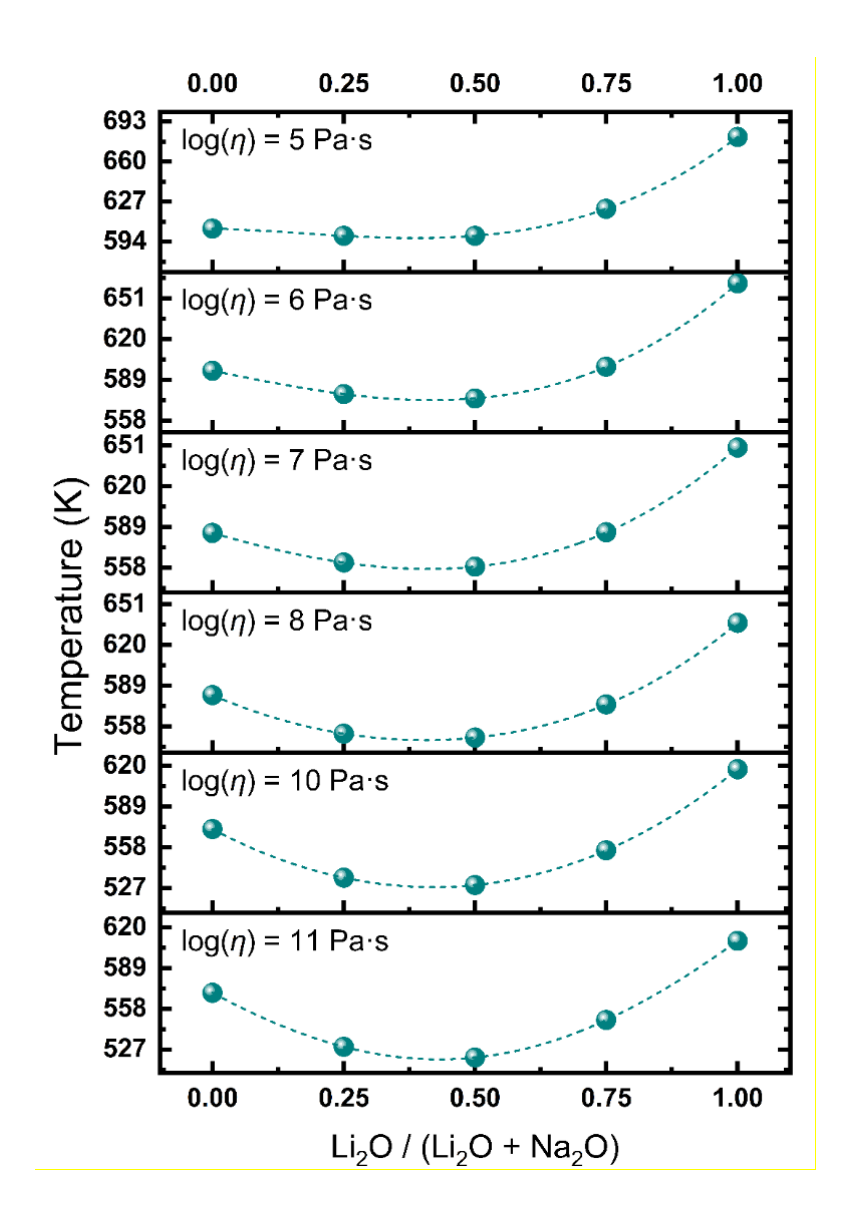


**Fig. 6.** Composition dependence of isokom (log  $\eta = 6, 7, 8, 10$  and 11 Pa·s) temperatures for Li<sub>x</sub>Na<sub>1-x</sub>PO<sub>3</sub> liquids from Fig. 5.

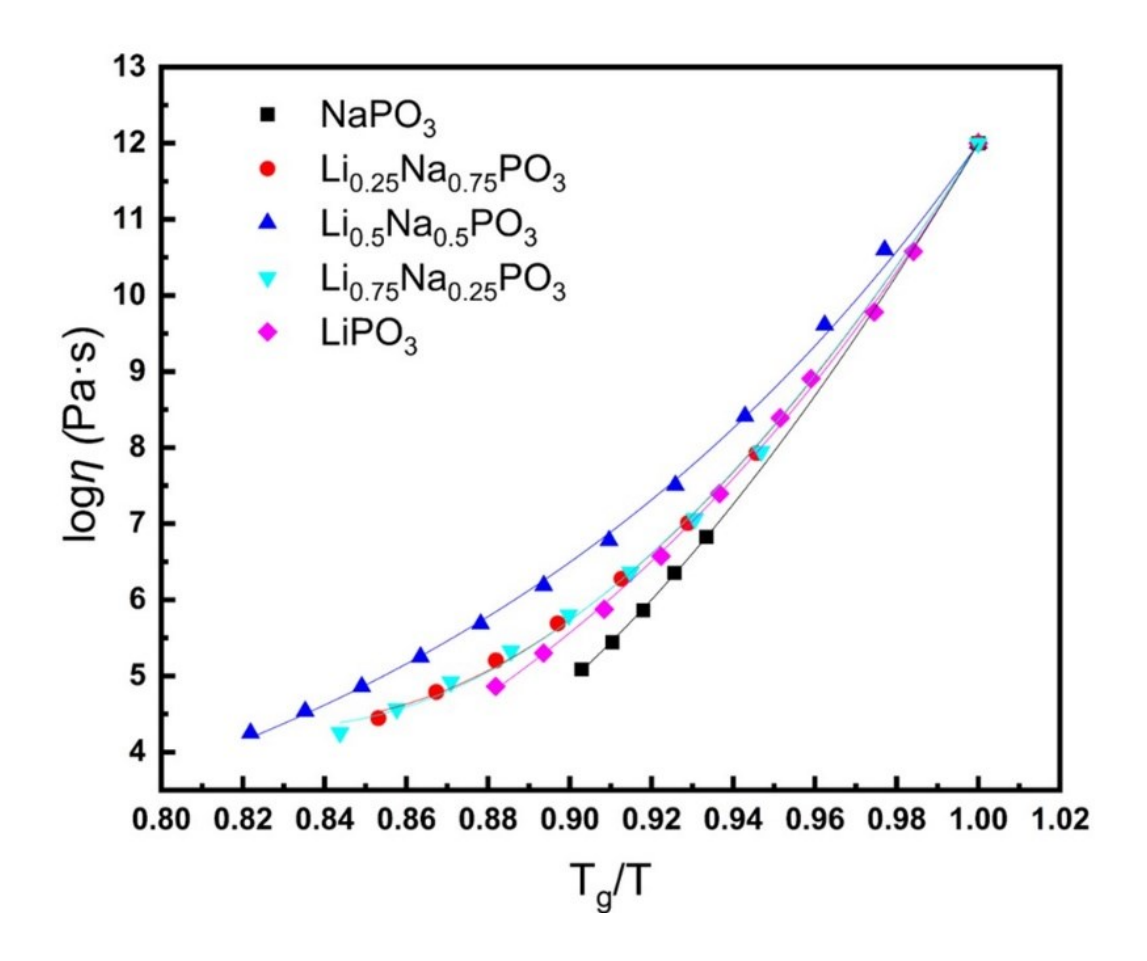


**Fig. 7.** Viscosity of Li<sub>x</sub>Na<sub>1-x</sub>PO<sub>3</sub> liquids as a function of reduced temperature  $(T_g/T)$ . Solid lines are fits of MYEGA equation to experimental data.

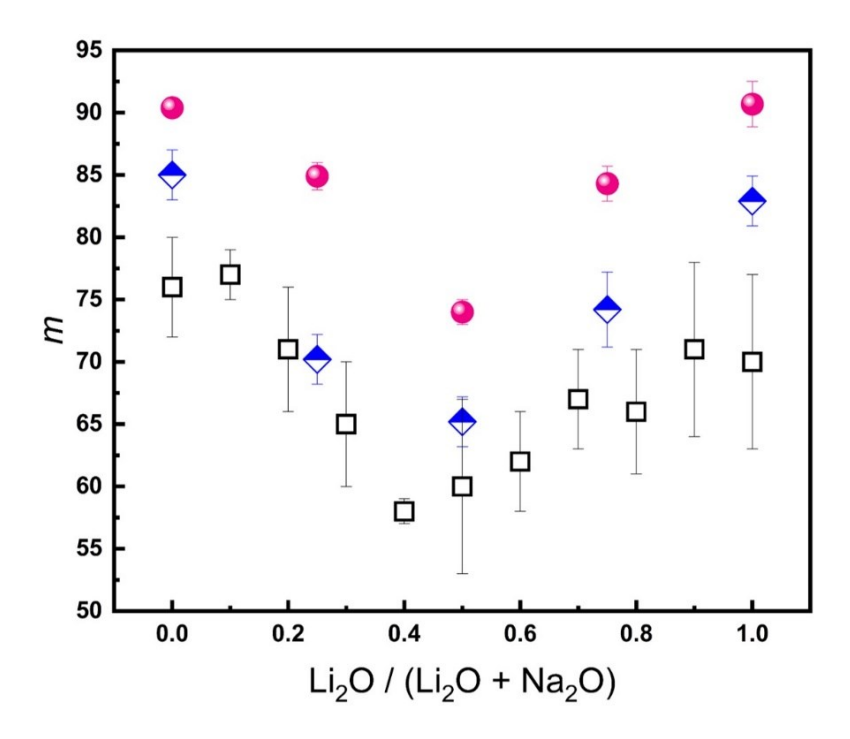


**Fig. 8**. Variation of kinetic (circles) and calorimetric (diamonds) fragility indices of Li<sub>x</sub>Na<sub>1-x</sub>PO<sub>3</sub> liquids with alkali composition measured in this study. Fragility data obtained from photon correlation spectroscopy (squares) as reported in a previous study are shown for comparison [12].

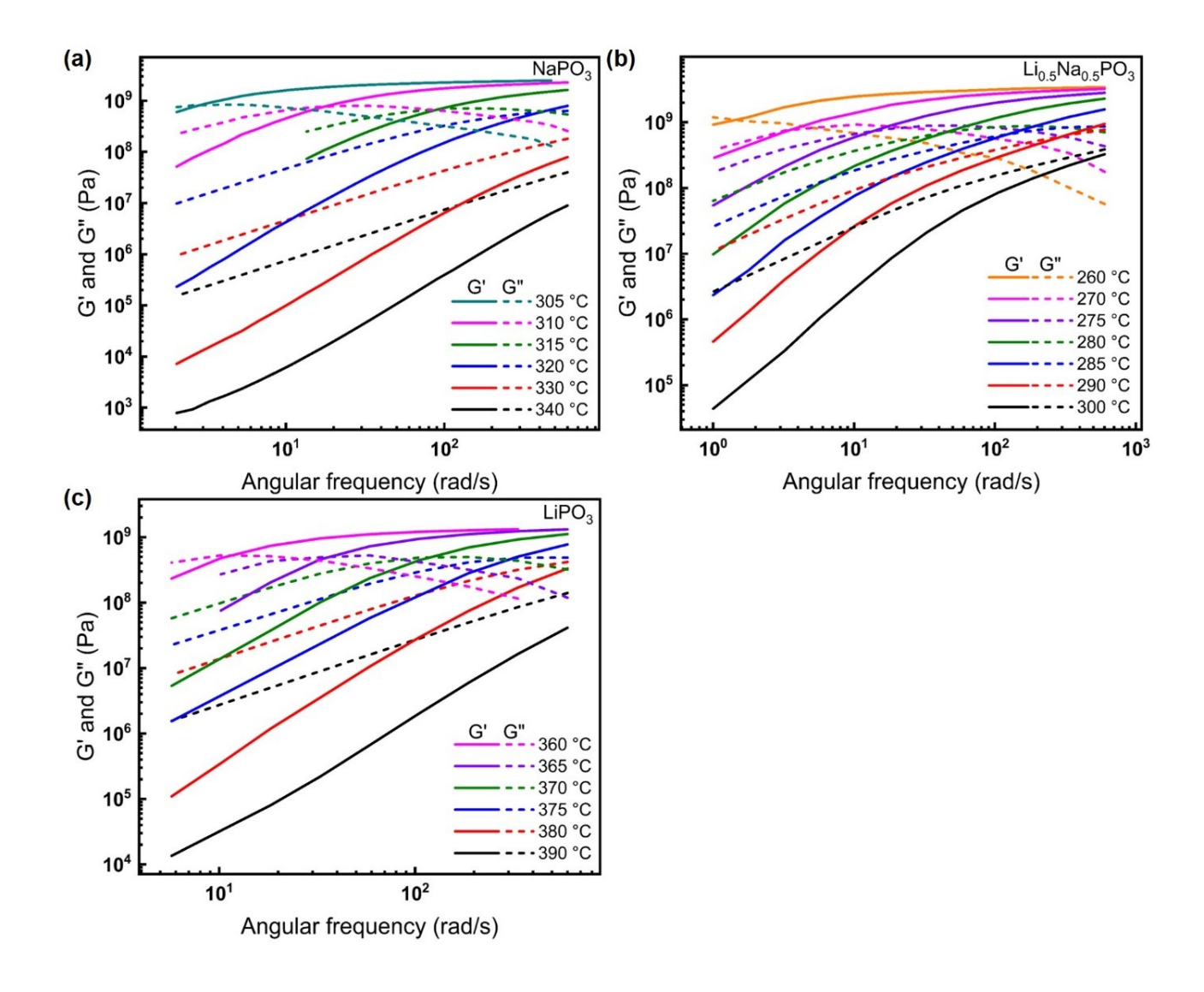


**Fig. 9.** Frequency dependence of G' (solid line) and G" (dotted line) at different temperatures for (a) NaPO<sub>3</sub>, (b) Li<sub>0.5</sub>Na<sub>0.5</sub>PO<sub>3</sub>, and (c) LiPO<sub>3</sub> liquids.

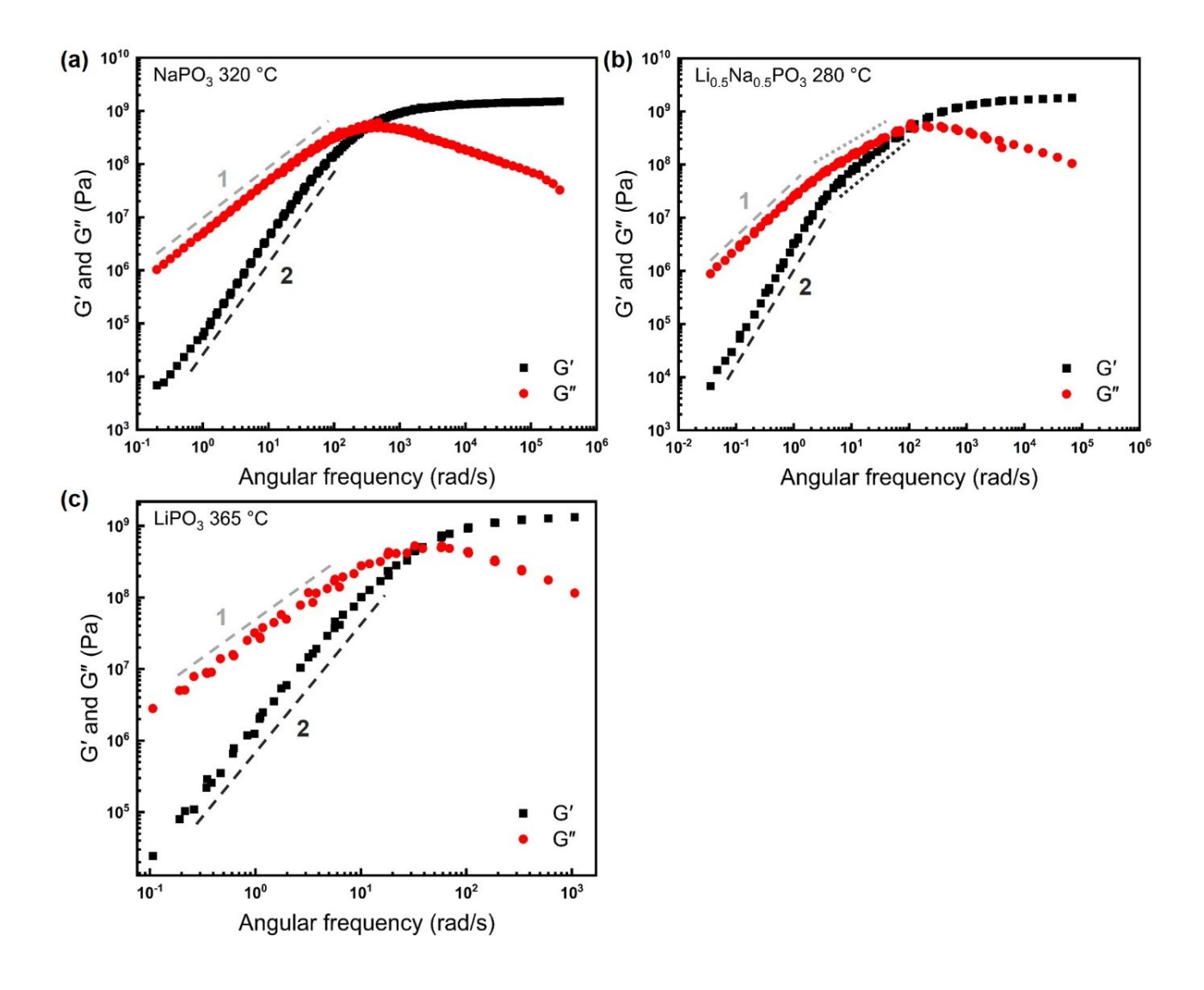


**Fig. 10**. Master curves of the angular frequency dependence of G' (squares) and G" (circles) for (a) NaPO<sub>3</sub>, (b) Li<sub>0.5</sub>Na<sub>0.5</sub>PO<sub>3</sub>, and (c) LiPO<sub>3</sub> liquids. Reference temperatures for TTS are listed in the inset. Data for NaPO<sub>3</sub> is from Xia *et al.* [33]. Dashed lines with slopes of 1 and 2 are guides to the eye.

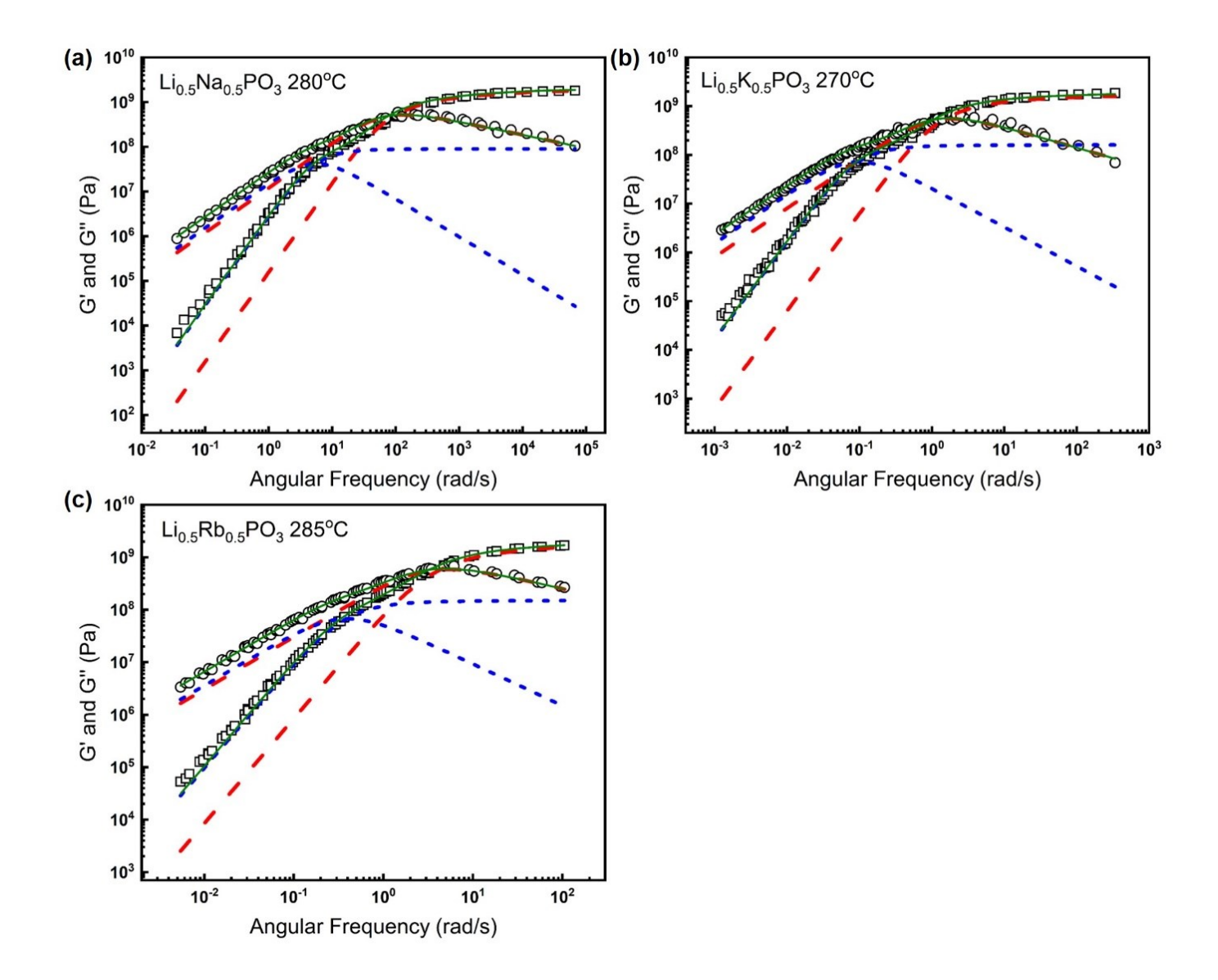


**Fig. 11.** Master curves of the angular frequency dependence of G' (squares) and G" (circles) for (a) Li<sub>0.5</sub>Na<sub>0.5</sub>PO<sub>3</sub>, (b) Li<sub>0.5</sub>K<sub>0.5</sub>PO<sub>3</sub>, and (c) Li<sub>0.5</sub>Rb<sub>0.5</sub>PO<sub>3</sub> liquids. Reference temperatures for TTS are listed in the inset. Two-component fits to these data with a slow (short dashed lines) and a fast (long dashed lines) relaxation process are shown.

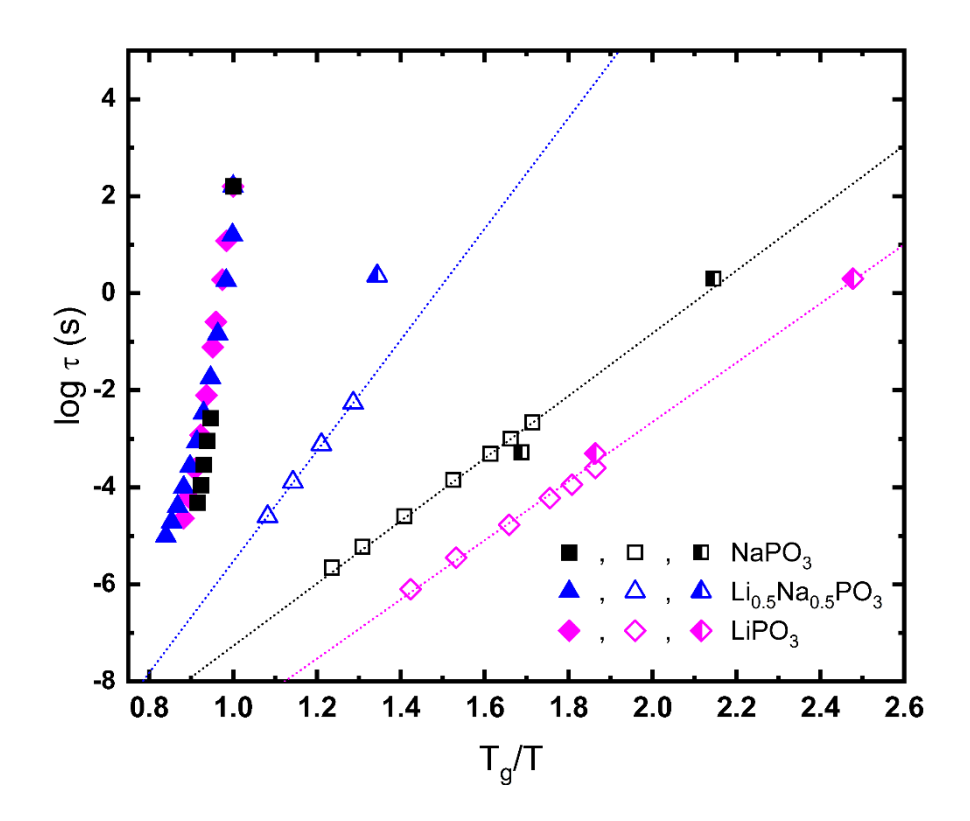


Fig. 12. Shear ( $\tau_{shear}$ , solid symbols) and conductivity ( $\tau_{cond}$ , open symbols) relaxation times as a function of reduced temperature  $T_g/T$  for Li<sub>x</sub>Na<sub>1-x</sub>PO<sub>3</sub> glasses and liquids. Half-filled symbols are internal friction relaxation times from van Ass and Stevels[27].

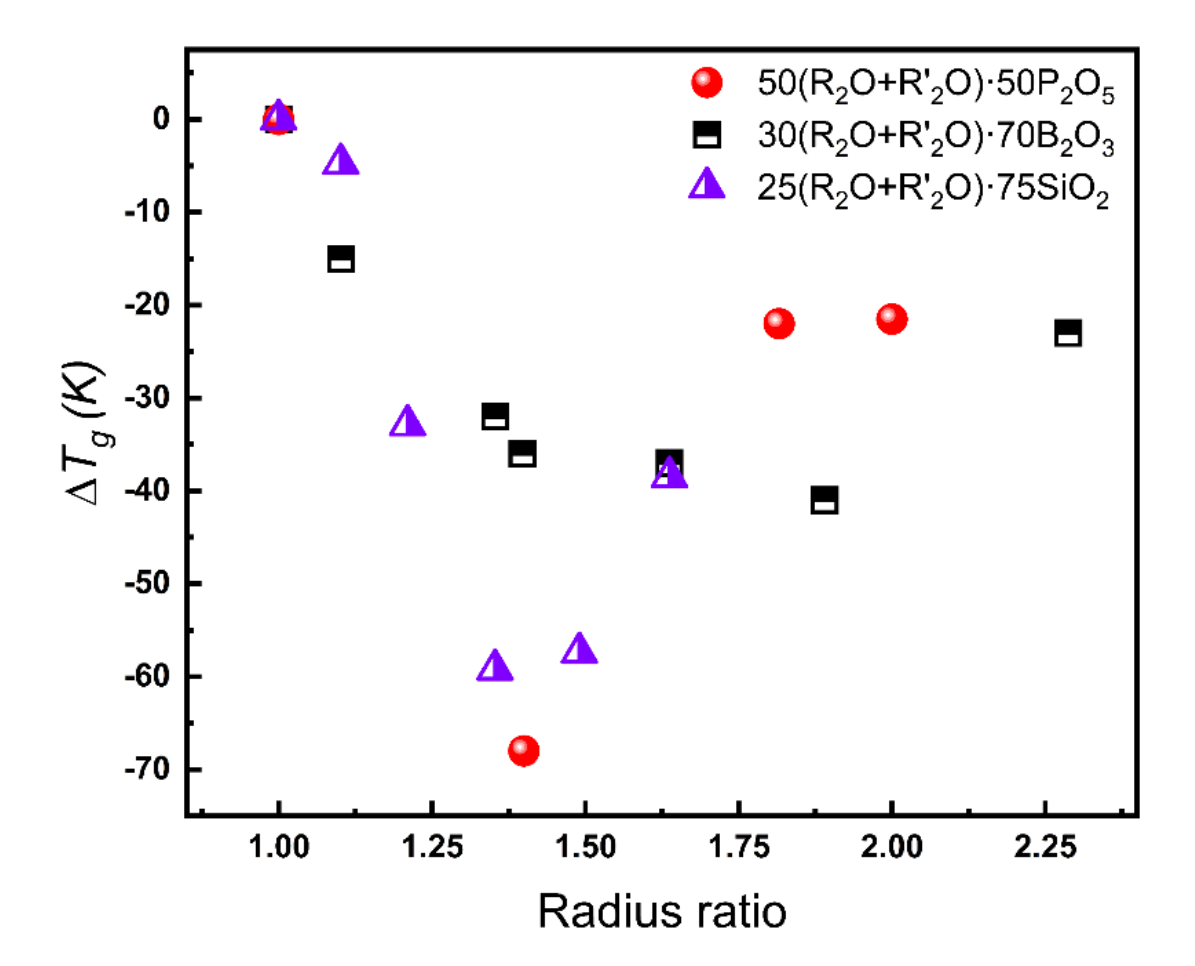
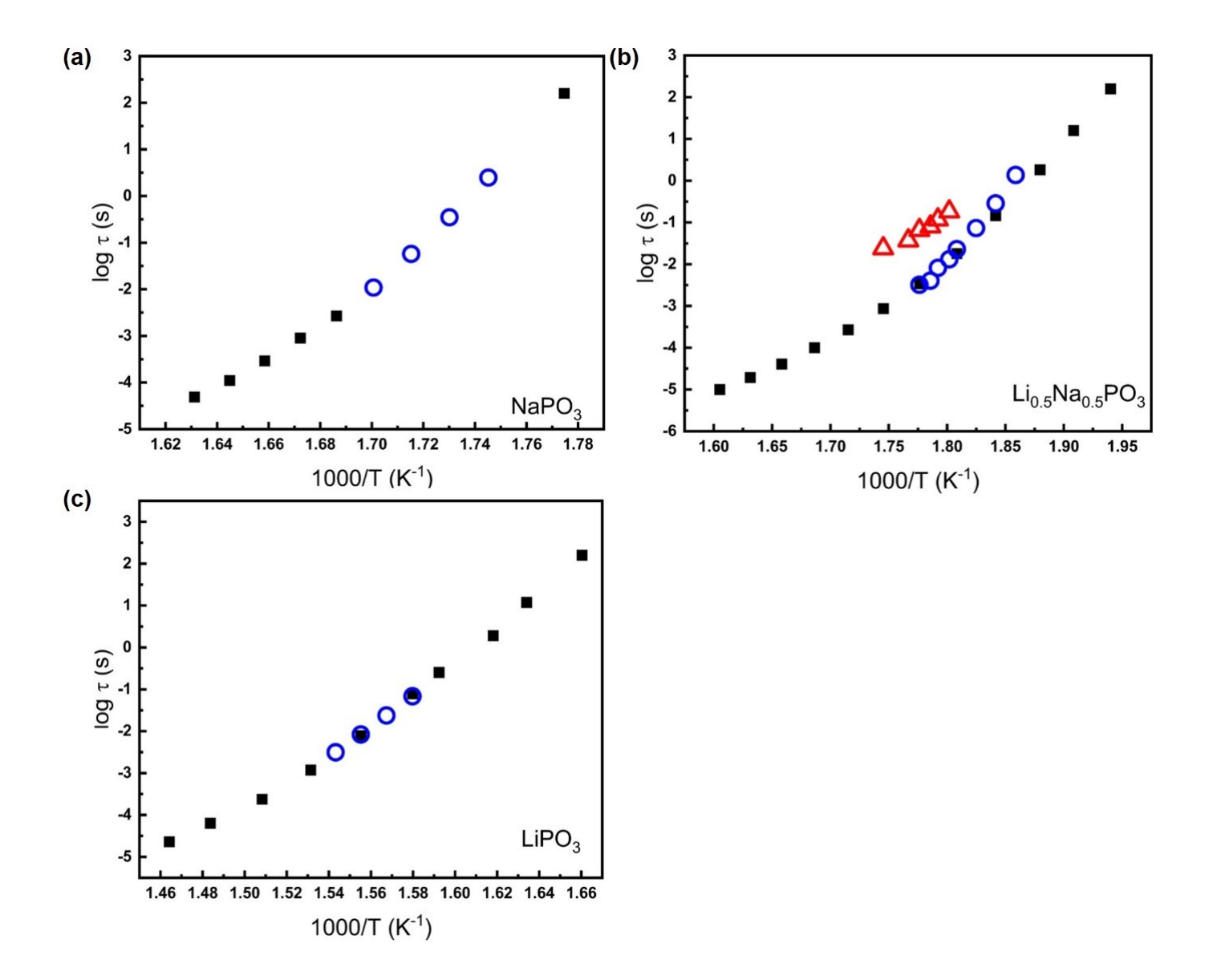
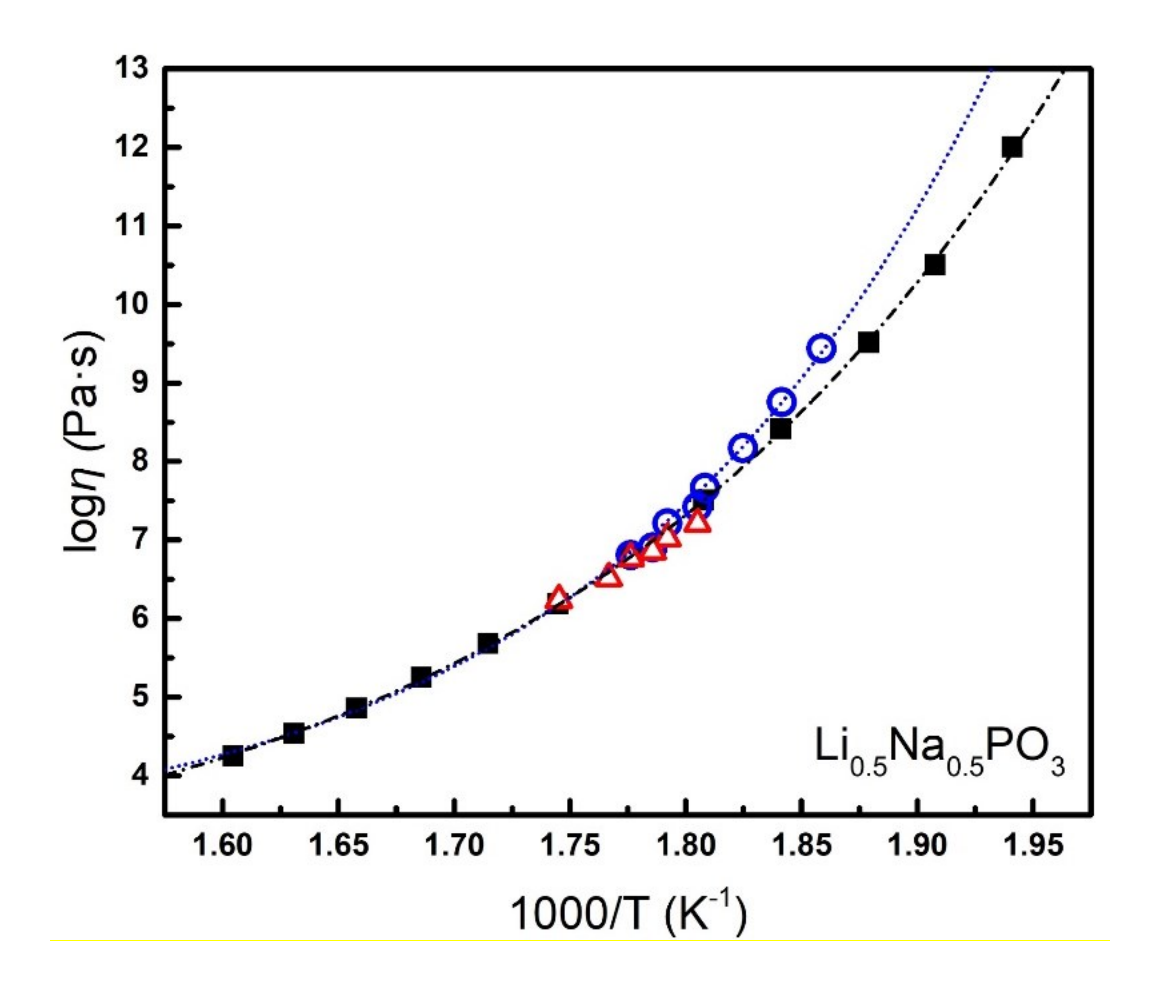


Fig. 13. Effect of radius ratio of constituent alkalis on the deviation from additivity in glass transition temperature  $\Delta T_g$  for mixed-alkali glasses. Data for alkali phosphates are from this study, while those for alkali borates (Li-Na, Li-K, Li-Cs, Na-K, Na-Cs and K-Rb) and alkali silicates (Na-K, Na-Rb, Na-Cs, K-Rb and K-Cs) are from Kuppinger and Shelby [11] and Shelby [10], respectively.



**Fig. 14**. Comparison between temperature dependence of shear relaxation time derived from viscosity (solid squares) and relaxation timescales obtained from viscoelastic spectra (circles and traingles) of (a) NaPO<sub>3</sub>, (b) Li<sub>0.5</sub>Na<sub>0.5</sub>PO<sub>3</sub>, and (c) LiPO<sub>3</sub> liquids. Circles and triangles correspond to the timescales of fast and slow dynamic processes, respectively, in the mixed-alkali Li<sub>0.5</sub>Na<sub>0.5</sub>PO<sub>3</sub> liquid. Note onset of decoupling between fast process and viscosity at the lowest temperatures and an increase in coupling of the latter with the slow process.



**Fig. 15.** Comparison between measured viscosity  $\eta$  (filled squares) of Li<sub>0.5</sub>Na<sub>0.5</sub>PO<sub>3</sub> liquid and predicted viscosity from fast segmental chain motion (circles) and slow P-O bond scission/renewal (triangles) processes, respectively. Lines through the datapoints are guides to the eye.